Lamellar ceramics of Ca_2SiO_4 prepared by mechanical activation of powders

A.B. Cabrera and M.E. Mendoza
Instituto de Física, Universidad Autónoma de Puebla,
Apartado Postal J-48, Puebla 72570, México.

Stoichiometric mixtures of calcium carbonate and silicon oxide have been mechanically activated by milling during several hours (29 and 50) previous to the solid state reaction, in order to obtain dicalcium silicate, Ca_2SiO_4. X-ray powder diffraction and differential thermal analysis studies show that the mechanical processing of the powders induces changes in the orientational uniformity of crystallites and the diminution of the decomposition temperature of the calcium carbonate. Microlamellar particles of β-Ca_2SiO_4 were obtained when the solid state reaction was achieved at 1450°C, whereas β-Ca_2SiO_4 and α'_L -Ca_2SiO_4 phases were obtained when the reaction took place at 1000°C. By means of the powder processing described in this work, we can prepare phase β-Ca_2SiO_4 without any chemical stabilizer and with an unusual lamellar morphology.

Keywords: Dicalcium silicate; mechanical activation; lamellar morphology.

Mezclas estequiométricas de carbonato de calcio y óxido de silicio fueron activadas mecánicamente mediante molido durante varias horas (29 y 50) antes de la reacción de estado sólido, con el fin de obtener silicato dicálcico, Ca_2SiO_4. Los estudios mediante difracción de rayos X en polvos y análisis térmico diferencial muestran que el procesamiento mecánico de los polvos induce cambios en la uniformidad de la orientación de los cristalitos y la disminución de la temperatura de descomposición del carbonato de calcio. Se obtuvieron partículas microlaminares de β-Ca_2SiO_4 cuando la reacción en estado sólido se realizó a 1450°C, mientras que cuando la reacción se efectuó a 1000°C, se obtuvo una mezcla de las fases β-Ca_2SiO_4 y α'_L -Ca_2SiO_4. Por medio del procesamiento de los polvos descrito en el presente trabajo, es posible obtener la fase β-Ca_2SiO_4 sin ningún estabilizador químico y con una morfología laminar poco usual.

Descriptores: Silicato dicálcico; activación mecánica; morfología laminar.

PACS: 81.20.Ev; 81.05.Je; 61.10.Nz

1. Introduction

Materials chemistry of silicates is a wide research field due to the richness of structure-properties relationships in these compounds. Dicalcium silicate, Ca_2SiO_4, is an interesting silicate because of its polymorphism. It presents five phases in the temperature interval between 30°C and 1500°C at 1 bar pressure [1]; the thermodynamically stable phases are α (space group P3_1c), α'_H (space group Pnma), α'_L (space group Pna2_1) and γ (space group Pbnm). There is also a low temperature metastable phase, the so-called β phase (space group P2_1/n) [2]. Recently a new phase was reported with space group P2_1/c [3].

Another reason that explains the interest in dicalcium silicate is that it is the second of the major components of ordinary Portland cement. In spite of being the most slowly reacting compound in the hydration of cement, its role in the hardening of cement is important because it is thought to be responsible for the longer term and continuing development of strength [4].

The typical method for synthesizing dicalcium silicate is the solid state reaction of oxides at high temperature [5]. Some other methods have been used successfully such as sol-gel, spray drying, evaporative decomposition of solutions, the Pechini process and thermal decomposition of hillebrandite [6-8].

Mechanical activation is a method that has been used to induce chemical reactions; this is possible because the milling process produce transformations in the reactants or in the self-heat sustaining reactions [9]. Different kinds of materials, from metallic to ionic, have been prepared using this method. In the case of oxides, there are some reports on rare earth oxides, zirconia, titanium oxide, etc. [10-12].

In this work we report a new method for synthesizing dicalcium silicate by the mechanical activation of calcium carbonate and silicon oxide powders, followed by a solid state reaction under milder conditions than usual in this type of reactions. X-ray powder diffraction, thermogravimetry, differential thermal analysis, and scanning electron microscopy studies, were performed to optimize the conditions to obtain the desired phase and also to characterize the silicate.

2. Experimental procedures

Dicalcium silicate was prepared by the solid state reaction of calcium carbonate and silicon oxide, according to the reaction: $2CaCO_3 + SiO_2 \rightarrow Ca_2SiO_4 + 2CO_2$.

Chemicals used were reactive grade (98%) and natural minerals. The starting materials were mechanically activated by milling during 29 or 50 hrs. This procedure was done in a rotary mill (150 rpm) with 70 cylinders of stabilized zirconia as milling media, occupying 45% in volume, in an alumina jar. In order to study the effect of the particle size in the mechanical activation process, particles of two sizes were prepared, 105 and 53 μm. We made this choice of sizes because the first one is a typical size used in the cement industry, and the second was to determine, by comparison, the

effect of reducing the powder size by half. Afterwards, the mixtures were used to prepare pellets by applying a pressure of 100 Kg cm^{-2}, in air at room temperature. Then the pellets were heated to 1000°C or 1450°C in alumina crucibles (1000°C) or zirconia crucibles (1450°C) in a muffle (Lindberg mod. 51844) for 1 hr., in air.

Thermogravimetric analysis (TGA) and differential thermal analysis (DTA) were employed to study the decomposition of calcium carbonate as a function of particle size and heating rate. These studies were done in simultaneous module (TA Instruments 2960), with heating rates of 5°C/min, 10°C/min, and 15°C/min up to 1000°C in air. X-ray powder diffraction (XRD) was used to quantitatively analyze the uniformity of orientation of powders and also to analyze their crystallinity after the milling process by means of the Full Width at Half Maximum (FWHM) of the pattern peaks. In addition, this method was used to identify the phases obtained after the mechanical processing and the solid state reaction. The phase identification was done by comparison with the Powder Diffraction Files (PDF) from the International Centre for Diffraction Data. XRD experiments were performed with an X-ray powder diffractometer (Bruker, AXS D5000)
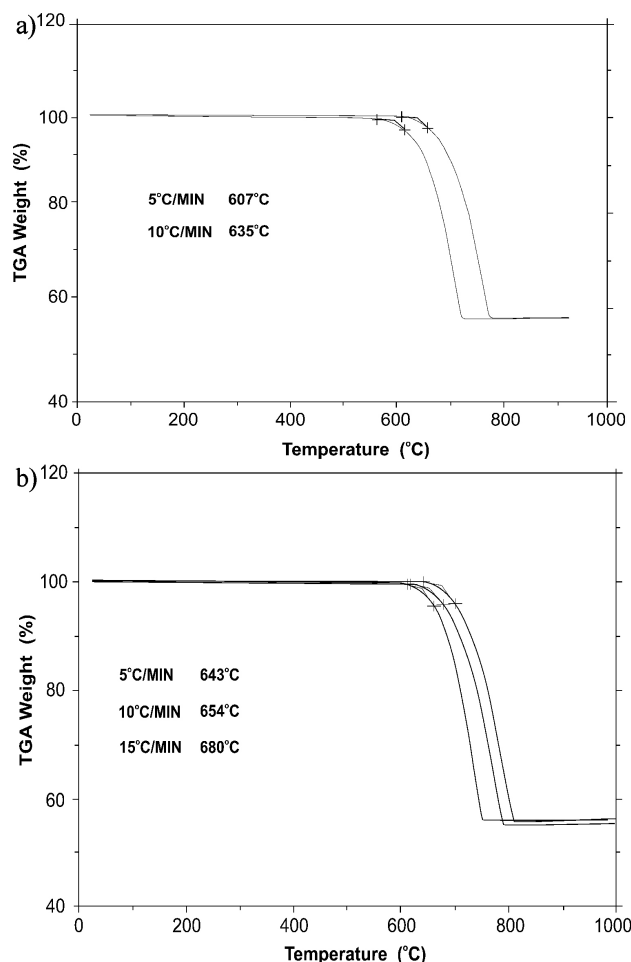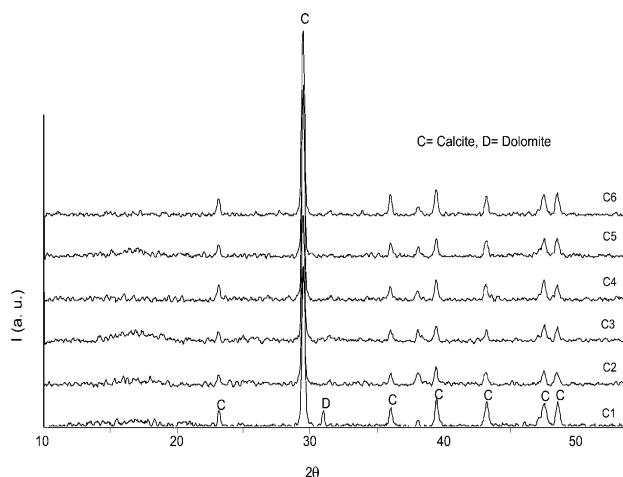
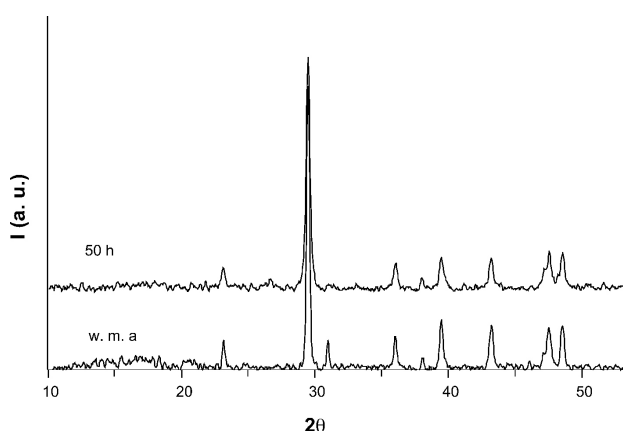

FIGURE 2. XRD patterns of several limestone after milling.

FIGURE 3. XRD patterns of limestone C1 without milling and after 50 h of mechanical treatment.

using Cu K$_\alpha$ radiation at room temperature. Morphological studies of the samples were done by scanning electron microscopy (SEM). SEM micrographs were obtained in a JSM 5400 LV (JEOL) system.

3. Results and discussion

3.1. Calcium carbonate decomposition

The reaction: $2CaCO_3 + SiO_2 \rightarrow Ca_2SiO_4 + 2CO_2$, consists of two steps. In the first, the decomposition of calcium carbonate occurs, producing calcium oxide; in the second, calcium oxide reacts with silicon oxide to produce dicalcium silicate. Our approach was to study firstly the decomposition reaction of calcium carbonate to determine the parameters that control it, then we used these results to optimize the solid state reaction of oxides.

The decomposition reaction $CaCO_3$ (s) $\rightarrow CaO$ (s) $+ CO_2$ (g) has an onset point at 661°C. The loss weight associated with the process is 43.97%. Since there is a structural relationship between calcium oxide and calcium carbonate, the reaction is of a topotactic nature [13].

FIGURE 1. TGA curves of thermal decomposition of CaCO$_3$ at heating rates of 15°C/min and 5°C/min in air. (a) limestone and (b) reactive grade.

TABLE I. Characteristics of limestone investigated in this study.

			TGA/DTA			
Sample	Heating rate [°C/min]	Features	Weight loss [%]	**TGA** Ti (decomposition) [°C]	Tf (decomposition) [°C]	**DTA** Tonset [°C]
CaCO$_3$	5	Calcium carbonate reactive grade 98% of purity.	45.0	643.2	751.3	626.2
	10		45.5	654.3	789.3	627.6
	15		45.5	680.0	808.6	671.6
C1	5	Darkest, very hard, grizzly colour. White regions of translucent appearance.	45.5	607.7	775.3	615.8
	10		45.5	635.1	829.2	634.4
C2	5	Whitest, with translucent shines; some black stains.	45.5	649.4	761.7	627.9
	10		45.5	674.9	804.5	645.8
	15		46.0	674.9	824.4	642.6
C3	5	With some very dispersed black points.	46.0	650.7	777.4	609.4
	15		46.0	688.0	833.6	655.4
C4	5	With some translucent white regions.	45.5	661.7	777.6	581.6
	10		46.0	697.1	809.0	664.7
	15		45.5	697.1	830.4	698.0
C5	5	Gray, it has a translucent white fringe.	45.0	665.3	781.5	577.1
	15		46.0	697.2	838.6	707.9
C6	5	Layered; brown, white and gray layers.	45.5	664.4	783.7	586.3
	15		46.0	704.2	839.8	711.3

We use natural samples, limestone (Tecali, México) as well as reactive grade samples (Monterrey 98%), in order to compare their decomposition process. Figure 1a and 1b show for samples milled to 105 μm, the curves of thermal decomposition at different heating rates. The onset point goes from 635 to 607°C for heating rates of 15 and 5°C/min respectively, in the case of natural samples (1a) , whereas it goes from 680 to 643°C/min for reactive grade samples (1b). Table I shows the characteristics and results obtained for several natural samples from the same geographical region. From these, it is clear that the kinetics of the process is strongly affected by the heating rate. Several studies on the kinetics of decomposition of calcium carbonate show that it depends strongly on the removal of carbon dioxide, which in turn is determined by its diffusion [13]. When the removal is under conditions of a controlled heating rate, the decomposition is guided by the transfer of thermal energy and/or gas diffusion within the sample, with the reaction interface playing a key role, because the features of the crystal symmetry of the reactant are maintained in the structure of the product in topotactic reactions [14].

In our case, the lowest heating rate can be associated with the lower temperature onset for the decomposition process in all the samples. Considering that all of them were milled for the same length of time (20 hrs.) and at the same particle size (105 μm), this suggests that the mechanical processing induces preferential orientation in powders, meaning that the

orientation of the reaction interface will be the proper one to optimize CO$_2$ diffusion.

Figure 2 shows the XRD patterns for several limestone samples after milling. They are in good agreement with the peaks reported in PDF for calcite (5-586); however, in sample C1, one peak corresponds to the dolomite phase, [Ca,Mg]CO$_3$. Of course, this indicates some traces of this phase. The presence of dolomite traces could also explain the DTA curves for sample C1, in which we observed the lowest onset of decomposition temperature, 607°C. Taking into account that the temperature reported for dolomite is considerably lower than that reported for calcite, 577°C and 661°C respectively [13], we can assume that dolomite is acting as flux.

As limestone C1 shows the lowest onset temperature of decomposition, we studied the effect of the milling time on these samples. If there were marks in the structure powders due to the mechanical processing, they must be present in the XRD pattern. Fig. 3 shows the XRD patterns of limestone without milling and after 50 hrs. of mechanical treatment.

In a comparison of both patterns, it is noticeable that in $2\theta \sim 26.5$ deg and $2\theta \sim 30.7$ deg, there are differences between them. It is observed that whereas in the samples milled we found a peak at $2\theta \sim 26.5$, it is absent in the samples without treatment. The identification of this peak was done by matching with PDF of CaO (28-775); its presence suggests that the mechanical processing induces the beginning of the

decomposition process of calcite. The peak at $2\theta \sim 30.7$ deg appears only in the samples without mechanical treatment; this corresponds to the dolomite phase, as was already shown in Fig. 2 for sample C1. Thus, the milling process also favors the decomposition of the traces of dolomite.

Moreover, in order to obtain some insight into the structural differences due to the processing, we obtained XRD patterns using a step scan of 0.5 deg/min. These data were compared with those of the randomly oriented calcite powder, PDF 5-0586 data.

The intensities of peaks in the standard XRD spectra of randomly oriented calcite powders (I^*_{hkl}) were normalized to quantitatively analyze the uniformity of orientation of calcite after milling (I_{hkl}). The percentage of calcite crystals in different orientations (hkl) was estimated according to the following equation [15]:

$$\%hkl = \frac{(I_{hkl}/I^*_{hkl})}{\sum_{hkl}(I_{hkl}/I^*_{hkl})} \times 100, \qquad (1)$$

Table II contains the calculated results using this equation. It was found that the uniformity of the orientation of calcite crystals changes with the mechanical processing. In non-treated samples the predominant planes are (024), (006), (104), (110) and (116), whereas in those milled they are (024), (006), (113), (104) and (012).

It should be noted that the percentage of calcite crystals in the (024) plane is dominant (49.3%) over the other orientations (below 8%) in non-treated samples, but in contrast, in the powders mechanically treated for 50 hrs., the percentage for the (024) plane decreases (33%) and that for (006) plane increases (17.8%).

Additional evidence of the consequence of mechanical processing in calcite powders was obtained by means of an analysis of XRD peaks studying their FWHM. Table III shows the FWHM of the XRD powder patterns of the aforementioned samples. It can be seen that in general, FWHM

TABLE II. XRD data of the crystallographic orientation of calcite powders before and after mechanical activation.

		w. m. a.		50h	
h k l	I^*_{hkl}	I_{hkl}	%hkl	I_{hkl}	%hkl
0 1 2	12.00	8.1	3.89	11.2	6.36
1 0 4	100.00	100.0	5.76	100.0	6.82
0 0 6	3.00	4.0	7.68	7.8	17.72
1 1 0	14.00	13.2	5.43	9.1	4.43
1 1 3	18.00	16.5	5.28	19.0	7.20
2 0 2	18.00	13.9	4.45	11.5	4.36
0 2 4	5.00	42.8	49.31	24.2	32.99
1 1 6	17.00	15.4	5.22	13.0	5.21
1 2 2	8.00	5.1	3.67	4.6	3.92
2 1 4	5.00	3.5	4.03	3.8	5.18
3 0 0	5.00	4.6	5.30	4.2	5.78

TABLE III. FWHM data of limestone powders without mechanical activation (wma) and after 50 h of milling.

	FWHM			
m. a. hrs.	Left Angle 2-Theta°	Right Angle 2-Theta°	Net Area CpsX2-Theta°	FWHM 2-Theta°
w. m. a.	22.76	23.60	4.115	0.218
50	22.72	23.40	3.417	0.276
w. m. a.	26.24	26.92	4.245	0.000
50	26.48	26.92	1.026	0.243
w. m. a.	28.88	30.08	54.020	0.264
50	28.92	30.08	49.210	0.298
w. m. a.	35.60	36.48	6.773	0.211
50	35.76	36.36	3.897	0.071
w. m. a.	39.20	39.92	6.847	0.041
50	39.16	39.96	5.332	0.064
w. m. a.	31.36	31.44	0.042	0.243
50	31.36	31.44	0.037	0.299
w. m. a.	42.84	43.72	6.178	0.274
50	42.88	43.72	4.630	0.312
w. m. a.	46.96	48.04	9.542	0.314
50	46.80	48.08	8.883	0.266
w. m. a.	48.24	49.08	6.628	0.330
50	48.36	49.08	4.316	0.295
w. m. a.	48.28	49.00	7.513	0.302
50	48.36	49.08	4.316	0.252

is larger for processed powders than for the non processed ones. It has been mentioned that this structural line broadening could be related to size broadening or strain broadening [16].

We estimate that the pressure exerted on calcite (Mohs hardness = 3) powders by two zirconia stabilized cylinders (Mohs hardness = 6) in the rotary mill (150 rpm) is about 1.2 GPa. Under these conditions, both, size-and strain-broadening could happen.

3.2. Dicalcium silicate synthesis

Stoichiometric quantities of calcium carbonate (limestone) and silicon oxide (sand) were mixed as required for the reaction $2CaCO_3 + SiO_2 \rightarrow Ca_2SiO_4 + 2CO_2$, and were milled in a rotary mill for 50 hrs. Figures 4a and 4b show the XRD patterns for samples with powder size 105 μm and 53 μm, respectively, after heating to 1000°C. The powders were mechanically processed for 50 hrs. In both cases the peaks correspond to Ca_2SiO_4. The identified phases were α'_L and β (PDF 36-0642 and 33-0302 respectively); however, their proportion was very different in each case. Quantitative determination of phases was calculated by measuring the normalized peak areas. In the sample of 105 μm, we found 68% of α'_L
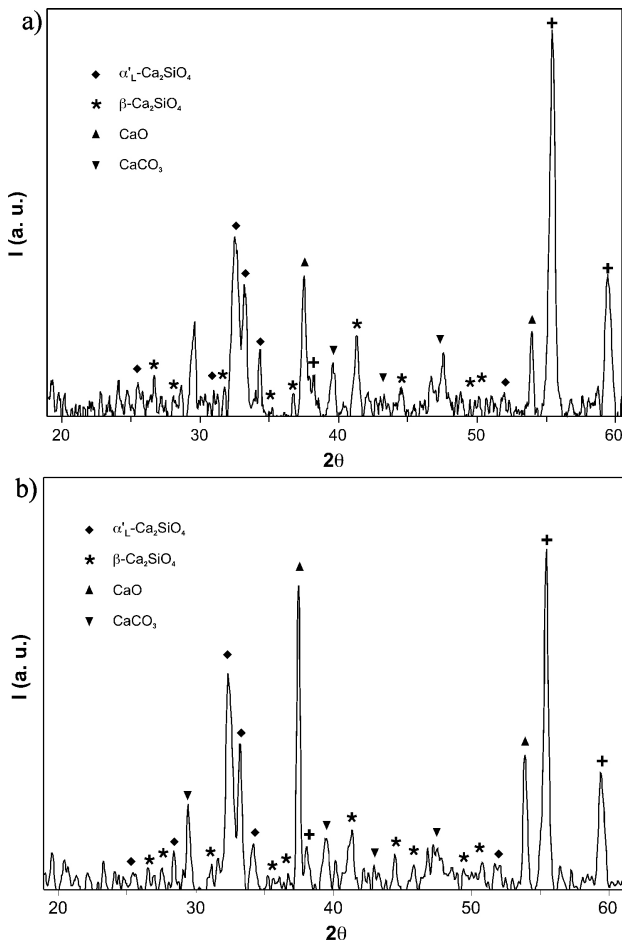
a)

b)

FIGURE 4. XRD pattern of the products after the solid state reaction between limestone and SiO_2. $T_{max} = 1000°C$. The reactants powders have been milled during 50 h, powder size (a) 105 μm, (b) 53 μm.

phase, 32% of β-phase, whereas for the sample of 53 μm, the respective percentages were 64 and 36%. There are also two intense peaks associated with calcium oxide and calcium
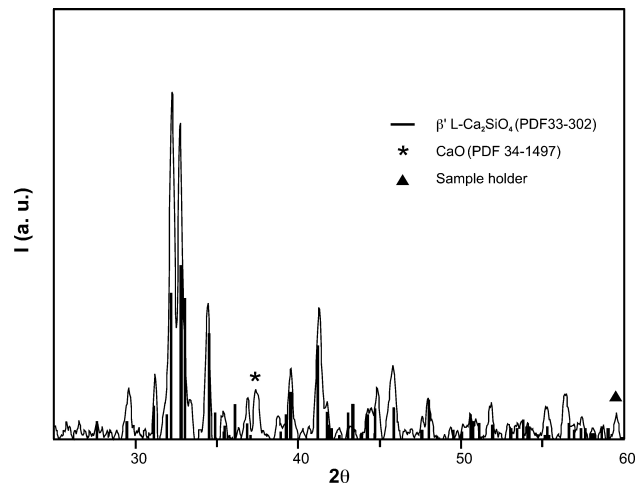

FIGURE 5. XRD pattern of the products of solid state reaction $CaCO_3 + SiO_2$. $T_{max} = 1450°C$, compared with PDF 33-302.

carbonate; their presence can be explained by the fact that the solid state reaction was incomplete at the work temperature, because the maximum temperature reached in these experiments was 1000°C. As the time of processing is the same, particle size is the main difference between these samples. It indicates that the formation of the β phase is favored by the shorter powder size. The presence of mixtures of α'_L and β phases is quite common in the synthesis of dicalcium silicate [1].

Figure 5 shows the XRD after a heat treatment at 1450°C in air during 1 hr. The major phase present was the ß-phase, in good agreement with the peaks in PDF for β-Ca_2SiO_4 (33-302). Also there are traces of CaO at 2θ= 37.4°, corresponding to the principal reflection in the PDF pattern for lime (37-1497).

The XRD patterns shown lead us to two important conclusions: the first one is that the mechanical treatment improves the reactivity of oxide powders. This is supported by
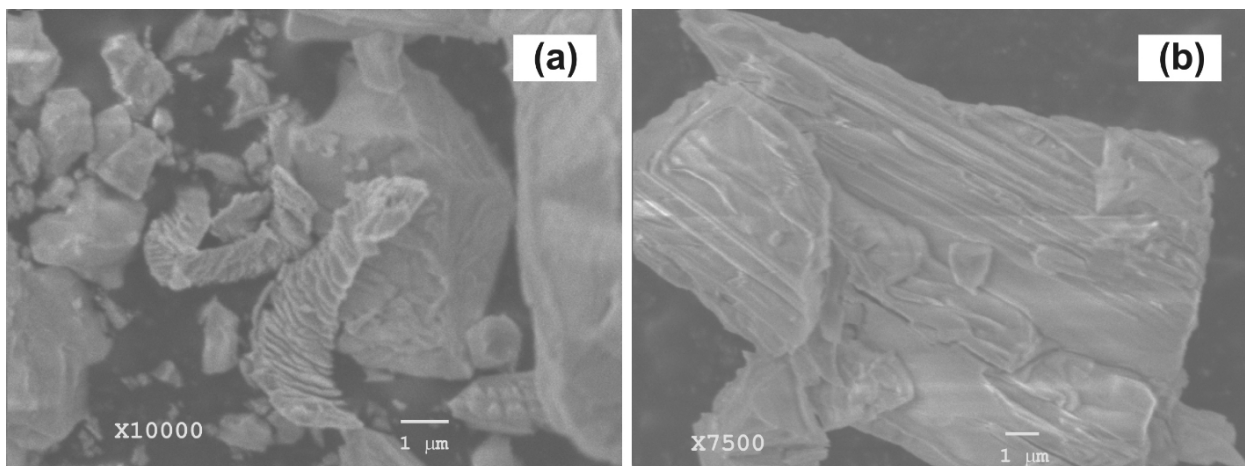

FIGURE 6. SEM micrographs of β-$CaSiO_4$ prepared by the solid state reaction of mechanically activated powders of $CaCO_3 + SiO_2$. $T_{max} = 1450°C$.

the fact that it is possible to obtain the mixtures of α'_L and β phases, even for samples calcined at low temperature (1000°C). The second is that β phase can be obtained without any chemical stabilizer at 1450°C.

Figure 6 shows SEM microphotographs of β-Ca$_2$SiO$_4$ crystals prepared by our procedure at T$_{max}$ = 1450°C. The morphology is lamellar; this is a very interesting result, because it has been reported to give needlelike fibers, when it is synthesized by spray drying or from hillebrandite [7,8]. Also spherical particles were obtained by the Pechini process [6]. Thus, it suggests that in our samples, the final morphology of β-dicalcium silicate is due to the fact that the morphology of calcite induced by the mechanical processing is preserved during the solid state reaction.

4. Conclusions

Mechanical processing of calcium carbonate changes the orientational uniformity of crystals as shown by XRD patterns.

Stoichiometric milled mixtures of calcium carbonate and silicon oxide were used to prepare pellets for the solid state reaction in order to obtain dicalcium silicate. A mixture of β and α'_L phases of dicalcium silicate was obtained when the reaction was conducted at 1000°C, whereas when the reaction was done at 1450°C, the β-phase was present showing the particles have an unusual lamellar morphology.

Acknowledgments

1. J.G. Fletcher, J.M.S. Skakle, I.R. Gibson, R.I. Smith, and F.P. Glasser, ISIS Experimental report (1997).

2. V.K. Peterson, Ph.D. Thesis, University of Technology, Sydney, Australia, (2003).

3. H. Toraya and S. Yamazaki, *Acta Cryst. B* **58** (2002) 613.

4. A.M. Neville, *Properties of Concrete*, 3th edition (Prentice Hall, New York, 1985).

5. M. Miyazaki, S. Yamazaki, K. Sasaki, H. Ishida, and H. Toraya, *J. Am. Ceram. Soc.* **81** (1998) 1339.

6. S.H. Hong and J.F. Young, *J. Am. Ceram. Soc.* **82** (1999) 1681.

7. L. Nettleship, J.L. Shull Jr., and W.M. Kriven, *J. Eur. Ceram. Soc.* **11** (1993) 291.

8. K. Sasaki, H. Ishida, Y. Okada, and T. Mitsuda, *J.Am. Ceram. Soc.* **76** (1993) 870.

9. E. Gaffet *et al.*, *J. Mater. Chem.* **9** (1999) 305.

10. G.B. Schaffer and P.G. McCormick, *Appl. Phys. Lett.* **55** (1989) 45.

11. N.S. Bell, J. Cesarano III, J.A. Voigt, S.J. Lockwood, and D.B. Dimos, *J. Mater. Res.* **19** (2004) 1333.

12. V. Berbenni and A. Marini, *Z. Naturforsch.* **57 b** (2002) 859.

13. A.K. Galwey and M.E. Brown, *Thermal decomposition of ionic solids* (Elsevier, Amsterdam, 1999).

14. A K Galwey and M E Brown, *Handbook of thermal analysis and calorimetry*, Principles and Practice (Ed. M.E. Brown, Elsevier, Amsterdam, 1998) Vol. 1.

15. Q.S. Shen *et al.*, *J.Phys. Chem. B* **109** (2005) 18342.

16. J.G.M. van Berkum, A.C. Vermeulen, R. Deles, T.H. de Keijser, and E.J. Mittemeijer, *J. Appl. Cryst.* **27** (1994) 345.